# Measuring self-steepening with the photon-conserving nonlinear Schrödinger equation

**N. Linale[1, 4, *], P. I. Fierens[2, 4], J. Bonetti[1, 4], A. D. Sánchez[1, 4], S. M. Hernandez[3], and D. F. Grosz[1,4]**

[1] *Depto. de Ingeniería en Telecomunicaciones, Centro Atómico Bariloche, Comisión Nacional de Energía Atómica, Río Negro 8400, Argentina*
[2] *Grupo de Optoelectrónica, Instituto Tecnológico de Buenos Aires (ITBA), CABA 1106, Argentina*
[3] *Instituto Balseiro, Universidad Nacional de Cuyo, Bariloche, Río Negro 8400, Argentina*
[4] *Consejo Nacional de Investigaciones Científicas y Técnicas (CONICET), Argentina*
[*] *Corresponding author: nicolas.linale@cab.cnea.gov.ar*

**We propose an original, simple, and direct method to measure self-steepening (SS) in nonlinear waveguides. Our proposal is based on results derived from the recently introduced photon-conserving nonlinear Schrödinger equation (pcNLSE), and relies on the time-shift experienced by soliton-like pulses due to SS upon propagation. In particular, a direct measurement of this time shift allows for a precise estimation of the SS parameter. Furthermore, we show that such an approach cannot be tackled by resorting to the NLSE. The proposed method is validated through numerical simulations, in excellent agreement with the analytical model, and results are presented for relevant spectral regions in the near infrared, the telecommunication band, and the mid infrared, and for realistic parameters of available laser sources and waveguides. Finally, we demonstrate the robustness of the proposed scheme against deviations expected in real-life experimental conditions, such as pulse shape, pulse peak power, pulsewidth, and/or higher-order linear and nonlinear dispersion.** 

http://dx.doi.org/10.1364/ao.XX.XXXXXX

Self-steepening (SS) is a nonlinear effect responsible for the optical shock of ultrashort pulses which acquires singular relevance when analyzing the dynamics of broadband spectra, such as in the case of supercontinuum generation [1, 2], and with applications to optical front-induced transitions [3]. Self-steepening is customarily introduced in pulse propagation models through a first-order approximation of the frequency dependence of the medium nonlinear coefficient. Known also as the 'shock term', $\tau_{sh}$, its relevance in the context of the modeling of supercontinuum generation was noted by Kibler, Dudley and Coen [4]. As it is explained in this work (see also Refs. [5, 6]), this shock term or SS parameter can be written as

$$\tau_{sh} = \frac{1}{\omega_0} + \frac{1}{n_2}\frac{dn_2}{d\omega} - \frac{1}{n_{eff}}\frac{dn_{eff}}{d\omega} - \frac{1}{A_{eff}}\frac{dA_{eff}}{d\omega}$$

where the derivatives are evaluated at $\omega = \omega_0$, $n_2$ is the nonlinear refractive index, $n_{eff}$ is the effective refractive index, and $A_{eff}$ the effective mode area. In a first-order approximation, the nonlinear coefficient of the waveguide is related to the SS parameter by $\gamma(\Omega) = \gamma_0(1 + \tau_{sh}\Omega)$, where $\Omega$ is the frequency detuning with respect to a conveniently chosen reference frequency $\omega_0$, and the SS parameter is usually given by $\tau_{sh} = \omega_0^{-1}$, an approximation that will become clearer in what follows.

In spite of its relevance, and to the extent of our knowledge, there is not much work in the literature on the direct measurement of the SS parameter. Indeed, most of the work has focused either on the numerical estimation or the measurement of the mode effective area, rather than on the direct measurement of $\tau_{sh}$. There are several reasons for this focus of literature on $A_{eff}$. As Kibler and colleagues note [4], the nonlinear refractive index $n_2$ is approximately constant in many relevant materials. Indeed, the frequency dependence of $n_2$ is negligible far from ultraviolet resonances in fused silica [7]. We must remark, however, that this observation does not hold, for instance, in the case of plasmonic materials that incorporate metal nanoparticles (MNPs), as waveguides doped with MNPs may exhibit a zero-nonlinearity wavelength (ZNW), giving rise to interesting new phenomena [8, 9]. Moreover, the frequency dependence of the effective mode index $n_{eff}$ is usually neglected as, in general, it is less relevant than that of the effective area.

Oftentimes, the estimation of the effective mode area dispersion is based on extensive numerical simulations or involved analytical calculations (see, e.g., [4, 10–16]). Nonetheless, the mode area can also be measured (see, e.g., [17–19]). A typical experimental procedure measures the spot size, either by registering the transverse mode with a camera or by some other method (see, e.g., [20]), and the effective mode area is calculated by fitting a Gaussian distribution [5, 10, 21], although such a fit is not valid in general [22].

Let us emphasize once more that the SS parameter is determined not only by the frequency dependence of the mode effective area, but also by the frequency dependence of the nonlinear refractive index. An interesting example of this type of dependence is found in the work of Panoiu, Liu and Osgood on silicon photonic nanowires [23, 24]. These authors show that

$\tau_{sh}$ can be more than 20 times greater than $\omega_0^{-1}$ for some wavelengths. Moreover, they prove that the frequency dependence of the third order susceptibility leads to significant changes in the SS parameter, even to the extent of making $\tau_{sh} < \omega_0^{-1}$.

Besides the lack of experimental schemes allowing for the direct measurement of the self-steepening parameter, a problem arises with the modeling of its influence. Propagation of light pulses in waveguides is usually modeled by the nonlinear Schrödinger equation (NLSE) [5]

$$\partial_z \tilde{A} = i\beta(\Omega)\tilde{A} + i\gamma(\Omega)\mathcal{F}\{|A|^2 A\}, \quad \textbf{(2)}$$

where $A = A(z,t)$ is the complex envelope of the electric field in the time domain, normalized such that $|A|^2$ is the optical power, and $\tilde{A} = \tilde{A}(z,\Omega) = \mathcal{F}[A(z,t)]$ where $\mathcal{F}$ stands for the Fourier transform. Coefficients $\beta(\Omega)$ and $\gamma(\Omega)$ are the linear and nonlinear dispersion profiles, respectively, and it is customary to express these profiles as Taylor expansions. It is worth noting that although the NLSE has proved to be adequate to model pulse propagation in a wide variety of cases, it is well known that it does not necessarily conserve some basic physical quantities such as the number of photons and the energy [6, 25, 26]. In particular, the photon number is preserved only if $\tau_{sh} = \omega_0^{-1}$, a fact often overlooked in the literature which poses a severe limitation when applying the NLSE to arbitrary nonlinear profiles $\gamma(\Omega)$. Let us define $s$ such that $\tau_{sh} = s\omega_0^{-1}$, i.e., $s$ is a measure of the deviation from the photon-conserving situation in the NLSE.

In order to overcome the aforementioned limitation of the NLSE, we have recently introduced a modified NLSE, the photon-conserving NLSE (pcNLSE) [27], that preserves both the energy and the number of photons in lossless waveguides. The pcNLSE reads

$$\partial_z \tilde{A} = i\beta(\Omega)\tilde{A} + i\frac{\omega r(\Omega)}{2}\mathcal{F}\{C^* B^2\} + i\frac{\omega r^*(\Omega)}{2}\mathcal{F}\{B^* C^2\}, \quad \textbf{(3)}$$

where $r(\Omega) = \sqrt[4]{\frac{\gamma(\Omega)}{\omega}}$, $\tilde{B} = r(\Omega)\tilde{A}$, and $\tilde{C} = r^*(\Omega)\tilde{A}$.

It can be easily verified that the pcNLSE reduces to the NLSE when $\tau_{sh} = \omega_0^{-1}$ ($s = 1$), i.e., in the only case where the NLSE preserves physical quantities. For all other values of the SS parameter, however, the pcNLSE predicts different results. For instance, Fig. 1 shows results of the propagation of a short pulse, in a waveguide with $s = -1$, modeled with the pcNLSE (solid line) and the NLSE (dashed line). Not only the predicted evolution is markedly different but, also, the NLSE predicts an unphysical increase of the number of photons upon propagation, as shown in the bottom panel.

It is interesting to revisit work dealing with the influence of self-steepening on soliton propagation in fibers [28, 29]. It is found that the soliton experiences a time shift due to SS but, most remarkably, no shock occurs (in agreement with Ref. [5]). Based on this resilience of a soliton to self-steepening, one may ponder whether such unique feature could be used to measure the SS parameter itself. Since the NLSE will only conserve the photon number when $s = 1$, we turn to explore the effect of self-steepening on soliton propagation under the much less restrictive context of the pcNLSE, keeping in mind that by 'soliton' we are referring to the fundamental soliton solution of the NLSE with no self-steepening.

Results obtained with the pcNLSE are shown in Fig. 2 for different values of $s$, where we observe that not only the soliton preserves its shape but it is time-shifted depending upon the value of the SS parameter. For clearness, the time shift $\Delta_T$ is normalized to the pulse $1/e$ half-width, $T_0$.

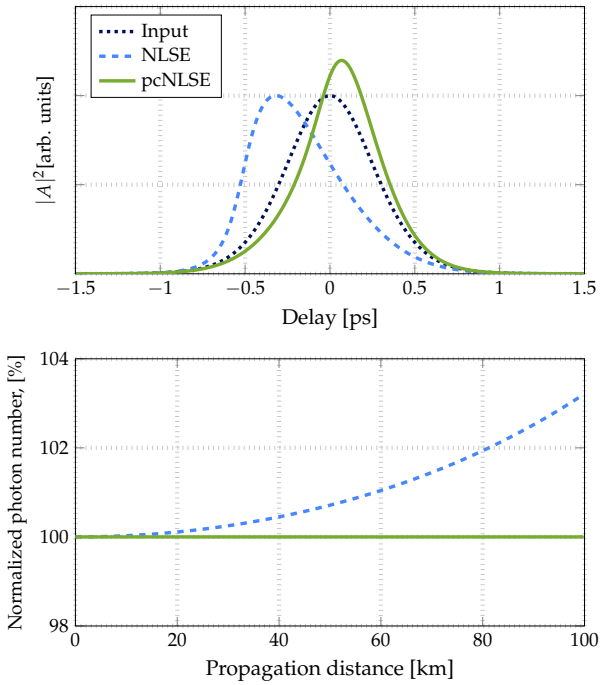


**Fig. 1.** The effect of self-steepening on the propagation of a short pulse in a waveguide with $s = -1$. Results with the NLSE (dashed line) and the pcNLSE (solid line). The pcNLSE preserves the photon number while the NLSE does not (bottom panel).

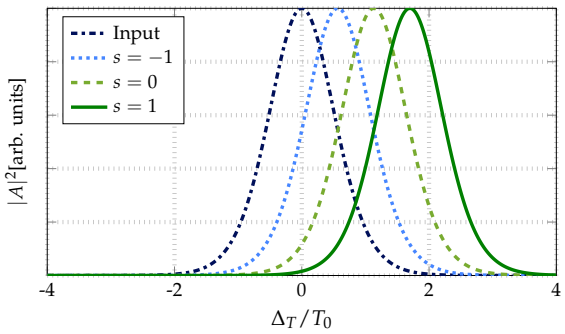


**Fig. 2.** Time shift experienced by a soliton due to self-steepening as predicted by the pcNLSE, and for different SS parameters: $s = -1$ (dotted line), $s = 0$ (dashed line), $s = 1$ (solid line); input pulse (dashed-dotted line). The time shift $\Delta_T$ is normalized to $T_0 = 100$ fs.

In order to find an analytical expression for the time shift, we must proceed in two steps. First, an approximation of Eq. 3 for narrowband pulses is developed and written in the time domain. Second, the method of moments [30–32] is applied assuming a hyperbolic secant pulse. As a result, it can be shown that (see Supplement 1 for details)

$$\Delta_T(z) = \frac{s+2}{3}\frac{\gamma_0 P_0 z}{\omega_0} = \frac{s+2}{3}\frac{\beta_2 z}{\omega_0 T_0^2}, \quad \textbf{(4)}$$

where $\gamma_0$ is the zeroth-order nonlinear coefficient, $\beta_2$ is the group velocity dispersion, and we have neglected higher-order dispersion. This equation is valid as long as the pulse remains unchirped along propagation, a condition that was verified, by

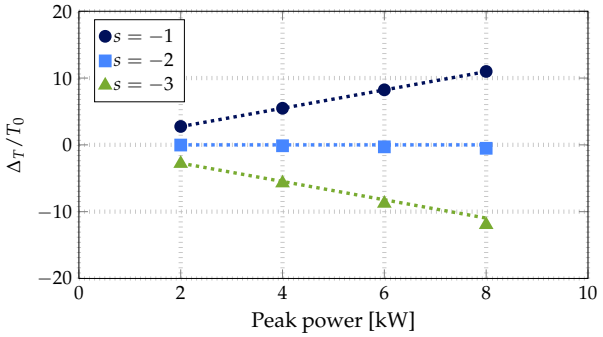


**Fig. 3.** Time shift experienced by a soliton, at $\lambda = 1550$ nm, vs. peak power and for different SS parameters: $s = -1$ (circles), $s = -2$ (squares), and $s = -3$ (triangles). Results from Eq. 4 are shown in dotted lines. Since $T_0 = 100$ fs, $\Delta_T \approx \pm 1$ ps for $s = \pm 1$ and a peak power of 8 kW.

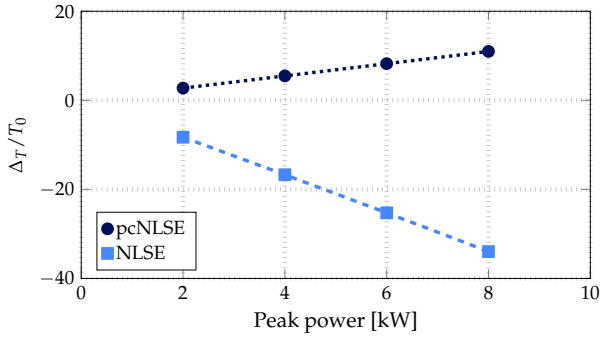


**Fig. 4.** Time shift vs. soliton peak power for $s = -1$ and same simulation parameters as in Fig. 3. (Circles) pcNLSE and (squares) NLSE. Results from Eq. 4 for the pcNLSE are shown in dotted line. The dashed line (NLSE) is a guide to the eye. Since $T_0 = 100$ fs, $\Delta_T \approx 1$ ps, for a peak power of 8 kW, in the case of the pcNLSE.

means of extensive numerical simulations, when the input is a fundamental soliton for the NLSE, i.e., $\gamma_0 P_0 T_0^2/|\beta_2| = 1$.

Equation 4 suggests a direct and simple way to estimate the SS parameter, based on measuring the delay experienced by a soliton upon propagation in a nonlinear waveguide. Note also that this expression is in agreement with the delay obtained with the NLSE and from self-phase modulation (SPM) considerations, and for $s = 1$, given by $\Delta_T \approx \gamma_0 P_0 z/\omega_0 = \phi_{\max}/\omega_0$, where $\phi_{\max}$ is the maximum phase induced by SPM [5]. Although the delay estimated with the NLSE can be generalized for an arbitrary $s$ as $\Delta_T \approx s\gamma_0 P_0 z/\omega_0$, only the case of $s = 1$ corresponds to a physically sound photon-conserving situation, and thus the derived self-steepening parameter will not be reliable for any other value of $s$.

Following this line of thought, in Fig. 3 we show simulation results on the propagation of solitons with peak powers ranging from 2 to 8 kW, $T_0 = 100$ fs, and central wavelength $\lambda = 1550$ nm (all parameters entirely consistent with those of a femtosecond fiber laser) along a 500-m long fiber with $\beta_2 = -20$ ps$^2$km$^{-1}$ and $\gamma_0 = 1$W$^{-1}$km$^{-1}$, both coefficients typical of a standard single-mode fiber at 1550 nm. Also shown in the figure is the linear dependence of the time shift as obtained from Eq. 4. As we can see, there is an excellent agreement between numerical simulations and results obtained with the pcNLSE.

In a practical experimental setup, one may envision a scheme where the time shift $\Delta_T$ is measured by launching two pulses into the waveguide: A large amplitude pulse which is time-shifted due to self-steepening and a small amplitude pulse which is not, and thus provides a convenient reference. The delay between pulses can then be measured by techniques such as GRENOUILLE [33] and/or modern devices based on two-photon absorption detectors [34].

It is interesting to compare results on the time shift obtained with the pcNLSE with those from the NLSE. This is shown in Fig. 4, where the case of $s = -1$ from Fig. 3 is compared to its NLSE counterpart. The NLSE predicts a time shift of significantly different magnitude than that obtained with the pcNLSE and of opposite sign. This highlights the necessity of resorting to the latter equation in order to have a reliable estimate of the SS parameter. Note that when $s = 1$ both equations will yield the same results, as this is the only case where the NLSE preserves the photon number.

Next, we are interested in validating our proposal in different spectral bands of particular relevance; namely, the near-infrared (NIR) and the mid-infrared (MIR) bands. In Fig. 5 we show results of the propagation of femtosecond pulses at $\lambda = 800$ nm (top) and $\lambda = 2400$ nm (bottom), in both cases along a 10-m long fiber with a negative SS slope $s = -1$. In the NIR the chosen fiber parameters are those typical of a photonic-crystal fiber (PCF) with $D = 40$ ps nm$^{-1}$km$^{-1}$ and $\gamma_0 = 95$ W$^{-1}$km$^{-1}$; in the MIR the chosen parameters are those of a typical ZBLAN fiber with $D = 10$ ps nm$^{-1}$km$^{-1}$ and $\gamma_0 = 1$ W$^{-1}$km$^{-1}$ [35]. As it can be readily observed, Eq. 4 makes correct predictions in both cases.

We also explore the robustness of the proposed method against deviations expected in real-life experimental conditions, such as pulse shape, peak power, and pulsewidth. In the top panel of Fig. 5 we show results obtained when considering a Gaussian-shaped pulse instead of a *sech*. We observe a power-dependent departure from the time-shift as given by Eq. 4, but as the linear trend holds it still allows for an estimation of the SS parameter. In the bottom panel of Fig. 5 we show results when considering deviations from the fundamental soliton condition, $N = 1$; in practical terms, these could be due to either peak-power and/or pulsewidth uncertainties in an experimental setup. As it is apparent from the figure, results are still in excellent agreement with the model, thus supporting the applicability of the proposed method.

It is worthwhile pointing out that there could be an intrinsic sources of deviations arising from effects such as waveguide losses, higher-order linear ($\beta_3$) and nonlinear ($\gamma_2$) dispersion, and/or the Raman-induced soliton self-frequency shift (SSFS) [5]. The effect of loss can be neglected by using a waveguide shorter than its corresponding effective length. The additional delays produced by $\beta_3$ and/or SSFS have been calculated analytically by using the NLSE [5, 32] and these results can be shown to apply to the pcNLSE as well. As such, these contributions can be subtracted in straightforward fashion from the total time delay, leaving only the self-steepening contribution needed to obtain the SS parameter.

Finally, to assess the applicability of the proposed method to more general (higher-order) nonlinear profiles, Fig. 6 shows results for the propagation of solitons along a 500-m-long fiber with $s = 1$ (solid line) and $s = -3$ (dotted line), and $\gamma_2 = -30\gamma_0/\omega_0^2$W$^{-1}$km$^{-1}$. The higher-order nonlinear profiles are shown in the top panel of Fig. 6. Results for the time delay

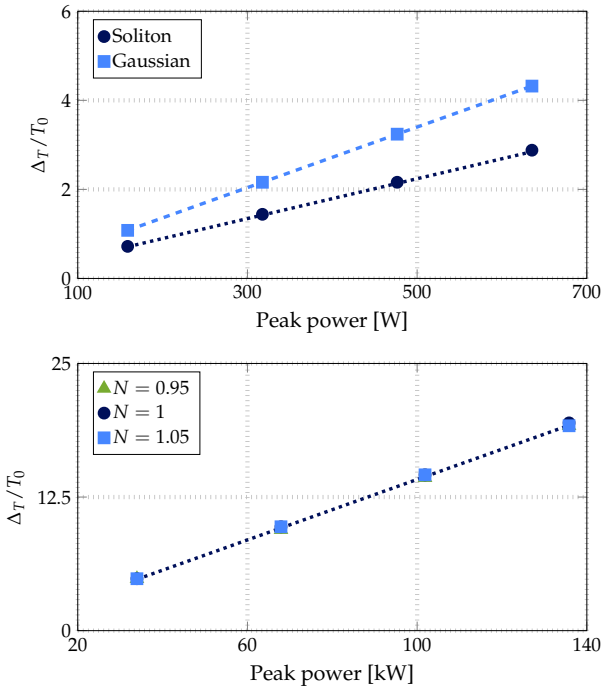


**Fig. 5.** Time shift vs. peak power with $s = -1$ as modeled with the pcNLSE in the NIR (top) and the MIR (bottom). Results from Eq. 4 are also shown (dotted lines). Effect of a Gaussian pulse shape (top, the dashed line is a guide to the eye). (Bottom) Effect of the deviation from the fundamental soliton condition $N = 1$. Since $T_0 = 30$ fs, $\Delta_T \approx 0.5$ ps, for a peak power of 130 kW, in the MIR case.

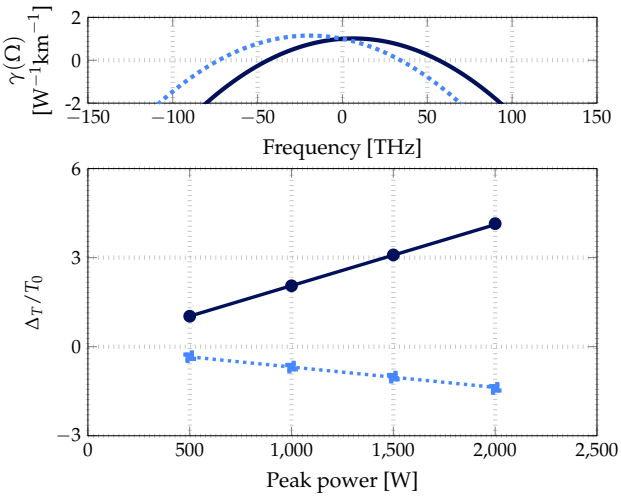


**Fig. 6.** (Top) Nonlinear profiles. (Bottom) Time shift experienced by a soliton, at $\lambda = 1550$ nm, vs. peak power in a fiber with $\gamma_2$, $s = 1$ (solid line) and $s = -3$ (dotted line). $T_0 = 200$ fs at 500 W.

shown in Fig. 6 are still in excellent agreement with the model.

In conclusion, we proposed an original, simple, and direct method to measure self-steepening in nonlinear waveguides based on results derived from the recently introduced photon-conserving nonlinear Schrödinger equation. Numerical results, in excellent agreement with the analytical model, were presented for relevant spectral regions in the NIR, MIR, and the telecommunication band. Finally, we showed the robustness of the proposed method against deviations expected in real-life experimental conditions, such as pulse peak power, shape, and width.

The authors declare no conflicts of interest.

See Supplement 1 for supporting content.

## REFERENCES


1. L. Zhang, Y. Yan, Y. Yue, Q. Lin, O. Painter, R. G. Beausoleil, and A. E. Willner, Opt. Express **19**, 11584 (2011).
2. B. Barviau, B. Kibler, and A. Picozzi, Phys. Rev. A **79**, 063840 (2009).
3. M. A. Gaafar, T. Baba, M. Eich, and A. Y. Petrov, Nat. Photonics **13**, 737 (2019).
4. B. Kibler, J. Dudley, and S. Coen, Appl. Phys. B **81**, 337 (2005).
5. G. P. Agrawal, "Nonlinear fiber optics," in *Nonlinear Science at the Dawn of the 21st Century*, (Springer, 2000), pp. 195–211.
6. K. J. Blow and D. Wood, IEEE J. Quantum Electron. **25**, 2665 (1989).
7. D. Milam, Appl. Opt. **37**, 546 (1998).
8. N. Linale, J. Bonetti, A. Sánchez, S. Hernandez, P. Fierens, and D. Grosz, Opt. Lett. **45**, 2498 (2020).
9. F. Arteaga-Sierra, A. Antikainen, and G. P. Agrawal, Phys. Rev. A **98**, 013830 (2018).
10. T. M. Monro, D. Richardson, N. Broderick, and P. Bennett, J. Light. Technol. **18**, 50 (2000).
11. G. Chang, T. B. Norris, and H. G. Winful, Opt. Lett. **28**, 546 (2003).
12. N. A. Mortensen, Opt. Express **10**, 341 (2002).
13. K. Saitoh, M. Koshiba, T. Hasegawa, and E. Sasaoka, Opt. Express **11**, 843 (2003).
14. S. A. Razzak and Y. Namihira, IEEE Photonics Technol. Lett. **20**, 249 (2008).
15. Y. Wang, X. Zhang, X. Ren, L. Zheng, X. Liu, and Y. Huang, Appl. Opt. **49**, 292 (2010).
16. S. Chugh, A. Gulistan, S. Ghosh, and B. Rahman, Opt. Express **27**, 36414 (2019).
17. W. S. Wong, X. Peng, J. M. McLaughlin, and L. Dong, Opt. Lett. **30**, 2855 (2005).
18. M. C. P. Huy, A. Baron, S. Lebrun, R. Frey, and P. Delaye, J. Opt. Soc. Am. B **27**, 1886 (2010).
19. M. C. P. Huy, A. Baron, S. Lebrun, R. Frey, and P. Delaye, J. Opt. Soc. Am. B **30**, 1651 (2013).
20. J. Streckert, Opt. Lett. **5**, 505 (1980).
21. D. Marcuse, J. Opt. Soc. Am. A **68**, 103 (1978).
22. M. Koshiba and K. Saitoh, Opt. Express **11**, 1746 (2003).
23. N. C. Panoiu, X. Liu, and R. M. Osgood, "Nonlinear dispersion in silicon photonic wires," in *2008 Conference on Lasers and Electro-Optics and 2008 Conference on Quantum Electronics and Laser Science*, (IEEE, 2008), pp. 1–2.
24. N. C. Panoiu, X. Liu, and R. M. Osgood Jr, Opt. Lett. **34**, 947 (2009).
25. A. D. Sánchez, P. I. Fierens, S. M. Hernandez, J. Bonetti, G. Brambilla, and D. F. Grosz, J. Opt. Soc. Am. B **35**, 2828 (2018).
26. A. Zheltikov, Phys. Rev. A **98**, 043833 (2018).
27. J. Bonetti, N. Linale, A. Sánchez, S. Hernandez, P. Fierens, and D. Grosz, J. Opt. Soc. Am. B **36**, 3139 (2019).
28. K. Ohkuma, Y. H. Ichikawa, and Y. Abe, Opt. letters **12**, 516 (1987).
29. J. De Oliveira, M. A. de Moura, J. M. Hickmann, and A. Gomes, J. Opt. Soc. Am. B **9**, 2025 (1992).
30. D. Marcuse, J. lightwave technology **10**, 17 (1992).
31. P.-A. Bélanger and N. Bélanger, Opt. communications **117**, 56 (1995).
32. Z. Chen, A. J. Taylor, and A. Efimov, JOSA B **27**, 1022 (2010).
33. S. Akturk, M. Kimmel, P. O'Shea, and R. Trebino, Opt. letters **29**, 1025 (2004).
34. J. Chen, W. Xia, and M. Wang, J. Appl. Phys. **121**, 223103 (2017).
35. D. Klimentov, N. Tolstik, V. Dvoyrin, V. L. Kalashnikov, and I. T. Sorokina, J. Light. Technol. **30**, 1943 (2012).

## FULL REFERENCES


1. L. Zhang, Y. Yan, Y. Yue, Q. Lin, O. Painter, R. G. Beausoleil, and A. E. Willner, "On-chip two-octave supercontinuum generation by enhancing self-steepening of optical pulses," Opt. Express **19**, 11584–11590 (2011).
2. B. Barviau, B. Kibler, and A. Picozzi, "Wave-turbulence approach of supercontinuum generation: Influence of self-steepening and higher-order dispersion," Phys. Rev. A **79**, 063840 (2009).
3. M. A. Gaafar, T. Baba, M. Eich, and A. Y. Petrov, "Front-induced transitions," Nat. Photonics **13**, 737–748 (2019).
4. B. Kibler, J. Dudley, and S. Coen, "Supercontinuum generation and nonlinear pulse propagation in photonic crystal fiber: influence of the frequency-dependent effective mode area," Appl. Phys. B **81**, 337–342 (2005).
5. G. P. Agrawal, "Nonlinear fiber optics," in *Nonlinear Science at the Dawn of the 21st Century,* (Springer, 2000), pp. 195–211.
6. K. J. Blow and D. Wood, "Theoretical description of transient stimulated raman scattering in optical fibers," IEEE J. Quantum Electron. **25**, 2665–2673 (1989).
7. D. Milam, "Review and assessment of measured values of the nonlinear refractive-index coefficient of fused silica," Appl. Opt. **37**, 546–550 (1998).
8. N. Linale, J. Bonetti, A. Sánchez, S. Hernandez, P. Fierens, and D. Grosz, "Modulation instability in waveguides with an arbitrary frequency-dependent nonlinear coefficient," Opt. Lett. **45**, 2498–2501 (2020).
9. F. Arteaga-Sierra, A. Antikainen, and G. P. Agrawal, "Soliton dynamics in photonic-crystal fibers with frequency-dependent kerr nonlinearity," Phys. Rev. A **98**, 013830 (2018).
10. T. M. Monro, D. Richardson, N. Broderick, and P. Bennett, "Modeling large air fraction holey optical fibers," J. Light. Technol. **18**, 50 (2000).
11. G. Chang, T. B. Norris, and H. G. Winful, "Optimization of supercontinuum generation in photonic crystal fibers for pulse compression," Opt. Lett. **28**, 546–548 (2003).
12. N. A. Mortensen, "Effective area of photonic crystal fibers," Opt. Express **10**, 341–348 (2002).
13. K. Saitoh, M. Koshiba, T. Hasegawa, and E. Sasaoka, "Chromatic dispersion control in photonic crystal fibers: application to ultra-flattened dispersion," Opt. Express **11**, 843–852 (2003).
14. S. A. Razzak and Y. Namihira, "Proposal for highly nonlinear dispersion-flattened octagonal photonic crystal fibers," IEEE Photonics Technol. Lett. **20**, 249–251 (2008).
15. Y. Wang, X. Zhang, X. Ren, L. Zheng, X. Liu, and Y. Huang, "Design and analysis of a dispersion flattened and highly nonlinear photonic crystal fiber with ultralow confinement loss," Appl. Opt. **49**, 292–297 (2010).
16. S. Chugh, A. Gulistan, S. Ghosh, and B. Rahman, "Machine learning approach for computing optical properties of a photonic crystal fiber," Opt. Express **27**, 36414–36425 (2019).
17. W. S. Wong, X. Peng, J. M. McLaughlin, and L. Dong, "Breaking the limit of maximum effective area for robust single-mode propagation in optical fibers," Opt. Lett. **30**, 2855–2857 (2005).
18. M. C. P. Huy, A. Baron, S. Lebrun, R. Frey, and P. Delaye, "Characterization of self-phase modulation in liquid filled hollow core photonic bandgap fibers," J. Opt. Soc. Am. B **27**, 1886–1893 (2010).
19. M. C. P. Huy, A. Baron, S. Lebrun, R. Frey, and P. Delaye, "Characterization of self-phase modulation in liquid filled hollow core photonic band gap fibers: erratum," J. Opt. Soc. Am. B **30**, 1651–1651 (2013).
20. J. Streckert, "New method for measuring the spot size of single-mode fibers," Opt. Lett. **5**, 505–506 (1980).
21. D. Marcuse, "Gaussian approximation of the fundamental modes of graded-index fibers," J. Opt. Soc. Am. A **68**, 103–109 (1978).
22. M. Koshiba and K. Saitoh, "Structural dependence of effective area and mode field diameter for holey fibers," Opt. Express **11**, 1746–1756 (2003).
23. N. C. Panoiu, X. Liu, and R. M. Osgood, "Nonlinear dispersion in silicon photonic wires," in *2008 Conference on Lasers and Electro-Optics and 2008 Conference on Quantum Electronics and Laser Science,* (IEEE, 2008), pp. 1–2.
24. N. C. Panoiu, X. Liu, and R. M. Osgood Jr, "Self-steepening of ultrashort pulses in silicon photonic nanowires," Opt. Lett. **34**, 947–949 (2009).
25. A. D. Sánchez, P. I. Fierens, S. M. Hernandez, J. Bonetti, G. Brambilla, and D. F. Grosz, "Anti-Stokes Raman gain enabled by modulation instability in mid-IR waveguides," J. Opt. Soc. Am. B **35**, 2828–2832 (2018).
26. A. Zheltikov, "Optical shock wave and photon-number conservation," Phys. Rev. A **98**, 043833 (2018).
27. J. Bonetti, N. Linale, A. Sánchez, S. Hernandez, P. Fierens, and D. Grosz, "Modified nonlinear schrödinger equation for frequency-dependent nonlinear profiles of arbitrary sign," J. Opt. Soc. Am. B **36**, 3139–3144 (2019).
28. K. Ohkuma, Y. H. Ichikawa, and Y. Abe, "Soliton propagation along optical fibers," Opt. letters **12**, 516–518 (1987).
29. J. De Oliveira, M. A. de Moura, J. M. Hickmann, and A. Gomes, "Self-steepening of optical pulses in dispersive media," J. Opt. Soc. Am. B **9**, 2025–2027 (1992).
30. D. Marcuse, "Rms width of pulses in nonlinear dispersive fibers," J. lightwave technology **10**, 17–21 (1992).
31. P.-A. Bélanger and N. Bélanger, "Rms characteristics of pulses in nonlinear dispersive lossy fibers," Opt. communications **117**, 56–60 (1995).
32. Z. Chen, A. J. Taylor, and A. Efimov, "Soliton dynamics in non-uniform fiber tapers: analytical description through an improved moment method," JOSA B **27**, 1022–1030 (2010).
33. S. Akturk, M. Kimmel, P. O'Shea, and R. Trebino, "Extremely simple device for measuring 20-fs pulses," Opt. letters **29**, 1025–1027 (2004).
34. J. Chen, W. Xia, and M. Wang, "Characteristic measurement for femtosecond laser pulses using a gaas pin photodiode as a two-photon photovoltaic receiver," J. Appl. Phys. **121**, 223103 (2017).
35. D. Klimentov, N. Tolstik, V. Dvoyrin, V. L. Kalashnikov, and I. T. Sorokina, "Broadband dispersion measurement of zblan, germanate and silica fibers in midir," J. Light. Technol. **30**, 1943–1947 (2012).